Egyptian Journal of Petroleum (2015) **24**, 145–154

HOSTED BY

ELSEVIER

Egyptian Petroleum Research Institute

Egyptian Journal of Petroleum

www.elsevier.com/locate/egyjp
www.sciencedirect.com

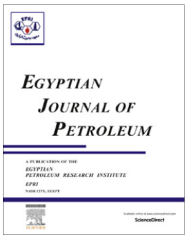

FULL LENGTH ARTICLE

Synthesis and characterization of polyurethane based on hydroxyl terminated polybutadiene and reinforced by carbon nanotubes

S.A. Shokry [a], A.K. El Morsi [c,*], M.S. Sabaa [b], R.R. Mohamed [b], H.E. El Sorogy [a]

[a] *Science and Technology Center of Excellence, El Salam City, Cairo, Egypt*
[b] *Department of Chemistry, Cairo University, El Giza, Egypt*
[c] *Department of Process Development, Egyptian Petroleum Research Institute, Egypt*

Received 13 February 2014; accepted 30 March 2014
Available online 19 June 2015

KEYWORDS

Multi-walled carbon nanotubes;
Polyurethane nanocomposites;
Reinforcement;
Microstructure;
Scanning electron microscopy;
Mechanical properties

Abstract Nanocomposites consisting of multi wall carbon wall carbon nano tubes MWCNT/polyurethane (PU) had been successfully prepared based on hydroxy terminated polybutadiene HTPB and the prepared MWCNT. The effect of concentration of prepared MWCNT and surface modified CNT on the morphology, mechanical reinforcement, and thermal properties of PU-based composites had been evaluated by FESEM, tensile testing, thermo gravimetric analysis TGA and differential scanning calorimeter DSC.

Polyurethane (PU) networks based on hydroxyl terminated polybutadiene (HTPB) and isophorone diisocyanate (IPDI) compound were prepared by a batch process. Two methods had been used to fabricate PU matrix/carbon nanotube nanocomposites: direct incorporation of unfunctional CNT (UCNT) into polymer matrices (noncovalent attachment) and in situ polymerization at their surface (covalent attachment).

TGA showed a much better improvement of thermal stability of the composites than pure PU. Glass temperature (Tg) increased due to high interaction of CNT with PU. Also Young's modulus increased. FESEM gave that the covalent attachment was better than noncovalent attachment for preparing PU/CNT composites.

1. Introduction

Carbon nanotube – Polyurethane Composite PU/MWCNT composites could be considered as ternary systems formed by the nanofiller, hard segments (HS) and soft segments (SS), each of which can vary in ratio, chemical composition and physical properties [1].

* Corresponding author.
E-mail address: drakilakamel158@yahoo.co.uk (A.K. El Morsi).
Peer review under responsibility of Egyptian Petroleum Research Institute.

http://dx.doi.org/10.1016/j.ejpe.2015.05.008

PU/MWCNT composites had been prepared by solution processing, melt-mixing, or in situ polymerization with different types of polyurethane and nanotube chemical characteristics. Moderate improvements of mechanical properties (such as tensile strength and Young's modulus) were systematically attained with contents of a few percent (~2–8 wt%) of nanofiller [2].

A polyurethane inserted multi-wall carbon nanotube (MWCNT) composite conductive film was prepared by in situ dispersed polymerization reaction using hydroxyl-terminated poly(butadiene-acrylonitrile) liquid rubber as a linear diol, toluene diisocyanate as a curative, ethylene glycol or glycerin or triethanolamine as a chain-extending agent and MWCNT as a conducive filler. The effect of various curing temperatures and chain-extending agents on vapor-induced electrical responsiveness of the conductive films was investigated [3].

Recent advances were used in nanotube dispersion technology to prepare composites based on polyurethane, with mass fractions of up to 80% polyethylene glycol functionalized nanotubes. Mechanical testing shows increases in Young's modulus compared to polyurethane films by up to 800 times [4].

A novel route was done to reduce the interfacial phonon scattering that was considered as the bottleneck for carbon nanotubes (CNTs) to highly improve the thermal conductivity of CNT/polymer composites [5].

The electroactive shape memory of carbon nanotube-filled polyurethane composites prepared by conventional blending, in situ and cross-linking polymerization, was studied in terms of the dispersion of the tubes. The covalently bonded tubes were homogeneously dispersed within the polyurethane by introducing carboxyl groups on the sidewall of the tubes and selecting a cross-linking polymerization method [6].

The multi-walled carbon nanotube (MWNT) reinforced thermoplastic polyurethane (TPU) nanocomposites were prepared through the melt compounding method followed by compression molding. The spectroscopic study indicated that a strong interfacial interaction was developed between carbon nanotube (CNT) and the TPU matrix in the nanocomposites. The mechanical properties of nanocomposites were substantially improved by the incorporation of CNTs into the TPU matrix [7].

The surface of multi-walled carbon nanotubes (MWCNTs) was modified by introducing acidic groups. Nanocomposites based on a polyurethane matrix (PU) containing chemically functionalized multi-walled carbon nanotubes (MWCNTs) had been shown to alter its mechanical performance depending on the nature of the surface functional groups on MWCNTs [8].

Polymer nanocomposites based on thermoplastic polyurethane (PU) elastomer and metal nanoparticle (Ag and Cu) decorated multiwall carbon nanotubes (MW-CNTs) through melt mixing process were prepared [9].

In this study PU – nanocomposites were prepared based on HTPB and the prepared MWCNT [10] of particle size (5.8, 36.9 nm) internal and external diameter, particle length 1–5 μm and no of shells 9. The effect of concentration of MWCNT and surface modified CNT on mechanical, thermal properties of PU – based composites had been evaluated by FESEM, tensile tests, TGA and DSC.

2. Experimental work

2.1. Materials

2.1.1. Hydroxyl terminated polybutadiene (HTPB)

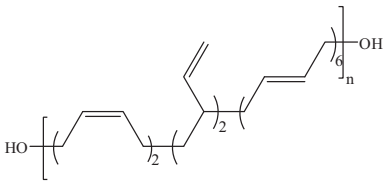

OH value	0.805 meq/gm
Viscosity at 30 °C	5630 cp
Density at 30 °C	0.9009 gm/ml
H_2O content	0.031%
Molecular weight	3800
Source	ARCO, USA

Microstructure of HTPB

Cis	20%
Trans	60%
Vinyl	20%

2.1.2. Isophorone diisocyanate (IPDI)

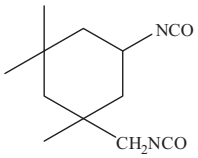

Name	5-isocyanate-1-(isocyanatomethyl)-1,3,3-trimethylcyclohexane
Assay	>98%; Sigma Aldrich, Germany
NCO value	8.1 meq/gm
Density	1.0614 gm/ml
Flash point	155 °C
Vapor pressure at 35 °C	0.04 Pa

CNT was prepared according to the method proposed in previous work [10]. The prepared CNT was modified to be used in this work.

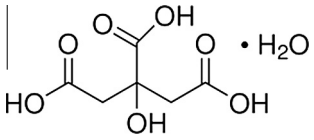

2.2. The modification of the CNT

2.2.1. Oxidation of carbon nanotube

The prepared CNT was treated with a mixture of concentrated sulfuric and nitric acids. MWCNTs were treated with a mixture of H_2SO_4 and HNO_3 with a weight ratio of H_2SO_4 to HNO_3 of 3:1 and a weight ratio of the mixed acid to the MWCNTs of 400:1 by stirring at 80 °C for 2 h to obtain acid-modified MWCNTs. Then, the mixture was vacuum-filtered through 0.2 μm Millipore PTFE membrane and washed with distilled water until the pH of the filtrate was 7.0. The filtered solid was dried under vacuum for 24 h at 60 °C, obtaining oxidized MWCNTs.

2.2.2. Reduction of CNT

The reduction of the oxidized MWCNTs was realized using lithium aluminum hydride ($LiAlH_4$), oxidized MWCNTs were dispersed in toluene by ultrasonication (in a water bath) for 30 min, and then $LiAlH_4$ was added gently by a ratio of 1:4. The solution was stirred for 1 h at room temperature, followed by adding 2.0 M hydrochloric acid by a ratio of 200:1 into the solution to remove the lithium and aluminum. The reduced MWCNTs were obtained by filtration of the solution and washed with toluene, absolute ethanol and acetone, and then dried in a vacuum oven at 80 °C overnight [11]. The complete modification of CNTs is illustrated in Scheme 1.

2.3. Synthesis of polyurethane and PU/MWCNT nanocomposite

The polyurethane networks based on HTPB and isophorone diisocyanate compound were prepared by a batch process. The process of synthesis of PU was as follows:

1. HTPB is weighted out according to the formulation as mentioned in Table 2.1 and is put in the reactor vessel.
2. The HTPB resin must be thoroughly degassed by evacuating the vessel in vacuum oven at 80–90 °C.
3. After an hour the prepolymer was cooled to 40 °C, then the evacuation was stopped and the weighed IPDI compound was added with a mechanical stirrer.
4. The mixture is stirred at 40 °C for ½ hour, air bubbles are removed by degassing under vacuum. After ½ hour the evacuation was stopped.

Table 2.1 The preparation formula of polyurethane and reinforced PU.

Sample	HTPB	IPDI	Purified MWCNT (%)	Modified MWCNT (%)
PU	120.4	10.7	–	–
PU/pCNT-0.5	120.4	10.7	0.5	–
PU/pCNT-1	120.4	10.7	1	–
PU/pCNT-2	120.4	10.7	2	–
PU/pCNT-4	120.4	10.7	4	–
PU/mCNT-0.5	120.4	10.7	–	0.5
PU/mCNT-1	120.4	10.7	–	1
PU/mCNT-2	120.4	10.7	–	2
PU/mCNT-4	120.4	10.7	–	4

5. The metal mold is lubricated by spraying a thin layer of fluorocarbon and then preheated to the curing temperature (60 °C).
6. The mixture without bubbles is poured into the preheated metal mold with dimensions 200 × 200 mm; the thickness of the polyurethane sheet is 5 mm.
7. Then the PU was cured in dehumidification oven at 60 ± 0.5 °C until the hardness or the polyurethane is steady for three days.

The polyurethane networks based on HTPB and reinforced by purified or modified CNTs were prepared as the following: CNT was dispersed in acetone to get a suspension system via an ultrasonicator for 2 h at room temperature, then adding the suspension slowly to HTPB under a mechanical stirring for 2 h. The matrix was heated to 80 °C for 12 h in vacuum oven. The dried mixture is cooled to 40 °C, then adding the weighed IPDI compound and the mixture was stirred with mechanical stirring for 0.5 h. Then the stirring was stopped. The closed mold is lubricated by spraying a thin layer of fluorocarbon and then preheated to the curing temperature (60 °C). The mixture was poured into the metal mold with 200 × 200 mm; the thickness of the polyurethane sheet is 5 mm. Then the PU was cured in dehumidification oven at 60 ± 0.5 °C until the hardness or the polyurethane is steady for three days. So the PU/CNT composite containing purified or modified tubes was obtained. The preparation of PU/CNT composites can be concluded in Scheme 2.

2.4. Characterization of polyurethane-CNT nanocomposites

2.4.1. Scanning Electron Microscopy (SEM) and Field Emission Scanning Electron Microscopy (FESEM)

The morphology of the pure PU of NCO/OH ratio of 10.06 was observed at low resolution by SEM (JEOL JXA-840A-JAPAN) operating at 20 kV. The samples were coated with

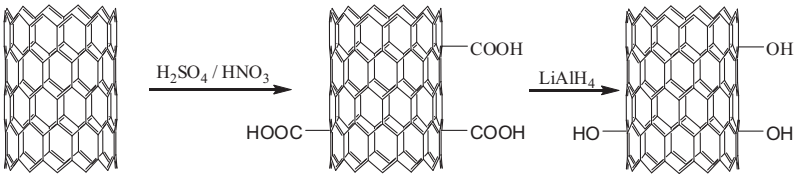

Scheme 1 Oxidation and reduction of CNT.

gold (Au) before the measurements to avoid charging problems. Acid treatment CNT, pure PU and PU nanocomposites were observed by FESEM (Quanta 250 Field Emission Gun FEI company, Netherlands) with accelerating voltage 30 K.V., magnification14x up to 1,000,000 and resolution for Gun.1n. The samples were coated with gold (Au) before the measurements to avoid charging problems.

CCD camera with special resolution reaching 0.14 nm.

2.4.2. Thermal Gravimetric Analysis

Thermal gravimetric profiles of the as prepared CNTs were recorded on TGA – Q 500 (TA Instrument, USA). Samples of approximately 5 mg in weight were heated in nitrogen atmosphere from 25 to 800 °C, at a rate of 10 °C/min.

2.4.3. Differential Scanning Calorimeter (DSC)

DSC Q 2000 (TA Instrument, USA) was used to measure the glass transition temperatures of the cured samples. Aluminum pans containing 5–9 mg of PU elastomer were carried out over a range of temperature from −70 to 150 °C at a heating rate of 10 °C min^{-1} in N_2 atmosphere (50 ml min^{-1}).

2.5. Determination of the mechanical properties

The specimens were in the form of dumbbells according to ASTM standard and procedure (D 638).

- Cutting of the elastomer samples for tensile test

After complete curing, the prepared elastomer sheet was cut to Dumbbell shape which was used for measuring the mechanical properties.

- Measurement of the mechanical properties

Stress/strain properties of the polyurethane were measured using Universal Test Machine Zwick 1487. The specimens were in the form of dumbbells according to ASTM standard and procedure (D 638).

For each sample, at least four were needed. Four pieces were tested and the average had to be calculated. The remaining sample could be used instead of any failed piece.

- Measurement of the hardness (Shore A)

The Shore A hardness of the nanocomposites was measured using an indentation hardness tester according to ASTM D2240 by using type A durometer. Hardness had been followed up starting from the third day after addition of the curing agent. It was measured daily until it gave the same reading all over three successive days. The hardness was measured at several points on the surface of the specimen. An average of eight measurements was taken as the result.

3. Results and discussion

3.1. Field Emission Scanning Electron Microscope (FESEM)

The dispersion of MWCNT [12] in matrix material greatly affected the properties of polymer/MWCNT composites. Here, FESEM was used to examine the dispersion of the pure MWCNT (pCNTs) and modified MWCNTs (mCNTs) in PU matrix. The fracture surface of the PU is presented in Fig. 3.1 while the fracture surfaces of PU/pCNT nanocomposites are shown in Fig. 3.2 and the fracture surfaces of PU/mCNT nanocomposites are shown in Fig. 3.3. The FESEM samples of cross-sections for the composite after tensile testing were obtained by brittle fracture of the composite. Fig. 3.1(A) shows low magnification SEM of fractured surface morphology of pure PU that exhibited a relatively smooth fracture surface. The high magnification image (FESEM) Fig. 3.1(B) showed the morphology of polyurethane domain.

Fig. 3.2(A–D) illustrates FESEM images of fracture surface of the PU/pCNT composite containing 0.5, 1, 2 and 4 wt% of pure MWCNTs. Fig. 3.2(A) shows the fracture of PU/pCNT-0.5 composite that revealed highly dispersed pCNTs and all of the CNTs had not been observed in the PU matrix. The pCNTs might be totally covered by polymer matrix [13].

The fracture surface of PU/pCNT-1 (Fig. 3.2(B)) showed a small number of individual CNTs pulled out of the PU matrix. The distribution of the pCNTs in the matrix was shown in white dots rather than small white lines that exposed from the matrix. A few CNT clusters appeared in the composite, as shown arrows in Fig. 3.2(B). High magnification (30,000×) of the marked zone (10,000×) inset of Fig. 3.2(C) was a close examination of the nanotube in PU/pCNT-2. Fig. 3.2(C) shows random dispersion of embedded MWCNT and localized CNT aggregations. PU/pCNT-2 composite had relatively more pCNT clusters (arrows in Fig. 3.2(C)); also the individual nanotubes have been observed. It was found that, Fig. 3.2(D) shows that many white small lines and white dots were scattered at the fracture plane of PU/pCNT-4 composite, indicating that the distribution of the pCNTs in the matrix of the composite was prone to random distribution on the cross-section of the composite. Large clusters were

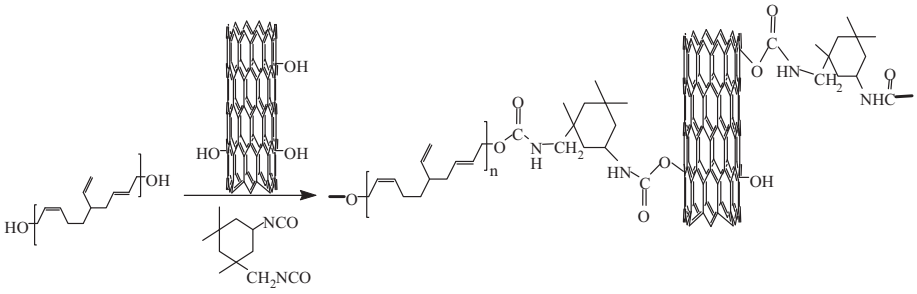

Scheme 2 Fabrication procedure of PU/MWCNT-IPDI composites.

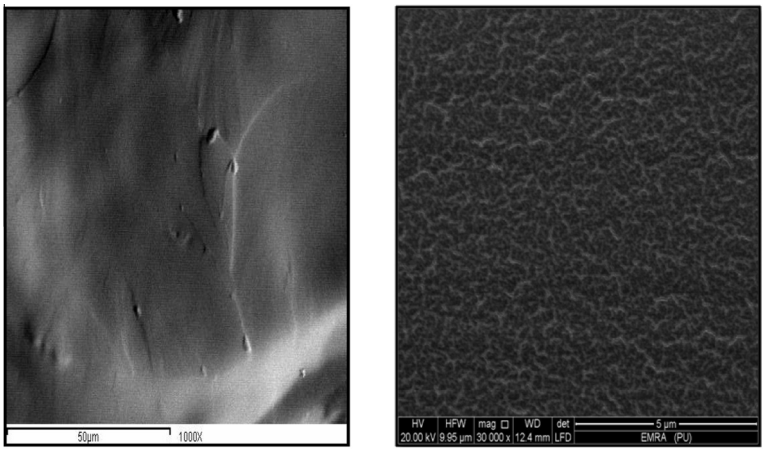

Figure 3.1 FESEM show the fracture surface and morphology of polyurethane domain of neat PU.

clearly found on the fractured surface of PU/pCNT-4. However FESEM data indicated that the pCNTs could be uniformly dispersed matrix under a lower concentration, while clusters easily form in the polymer matrix at higher concentration of pCNTs. [14].

The examination of the changes of the distribution between the pCNTs and mCNT in the composite was observed by FESEM. Here, FESEM was used to examine the morphology and dispersion of the mCNT in PU matrix, as shown in Fig. 3.3, where A, B, C, D were the SEM images of the composite containing 0.5, 1, 2, 4 wt% of mCNTs, respectively. CNTs appeared as bright points and lines in the micrographs. Fig. 3.3(A) shows that the bright points did not appear in the fracture surface of PU/mCNT-0.5. Closer examination of the nanotube revealed a thicker layer of PU that seemed to cover the CNTs surface, indicating some degree of wetting and phase adhesion. While Fig. 3.3(B–D) had shown that the PU-embedded mCNTs appeared as bright points and lines in the micrographs. The bright dots increased with respect to MWCNT content. The mCNTs were pulled out from the fractured surface. Increasing the amount of mCNTs up to 4 wt% in the nanocomposites resulted in dramatic changes in the structure of polyurethane, which exhibits near complete disappearance of domain structure of polyurethane (Fig. 3.3B–D). When small quantities of mCNTs (0.5 wt%) were used in the preparation of nanocomposites, the number of nanotubes was insufficient to noticeably influence the native domain structure of PU. By increasing the amount of mCNTs up to 8 times (4 wt%) and taking into account a good dispersion of nanotubes being achieved, the effective surface of mCNTs, which influence the native structure of polyurethane, becomes large enough to prevent the formation of soft domains within the frame of the polyurethane structure. The covalent bonding of the MWCNTs (i.e. CNT-OH) with PU or van der Waals interactions of the unfunctionalized areas of the MWCNT surface with polyurethane matrix should lead to improved disagglomeration of the nanotube bundles and the good dispersibility of MWCNTs into a polymer. It was attributed to the increase in polarity of the mCNTs by the functional groups and the interaction of the –OH group of CNTs with the isocyanate (–NCO–) group of the PU matrix. Most of the mCNTs in Fig. 3.3(B–D) were observed to be broken rather than just pulled out of the matrix under cleaving the samples, which also indicates that the interconnection of mCNTs with PU matrix is very strong.

3.2. Thermal Gravimetric Analysis (TGA)

Thermal stability of the PU was assessed by a TGA technique. Fig. 3.4 represents the thermogravimetric curves for neat PU, PU/pCNT and PU/mCNT nanocomposites. For all the samples, degradation was observed in two steps. The thermal degradation of PU generally occured in two stages. According to the degrading mechanism of PUs, the first stage was associated with the breakdown of the urethane linkage (–HN–COO–) to the original polyol and isocyanate. After that, the polyols and diisocyanates started to decompose, respectively. The polyol and isocyanate further undergo cleavage of the chemical bonds to form small molecules (primary amine, alkene, aldehyde, ketone, carbon dioxide, water). It should be noted that the present MWCNT content was 0.5, 1, 2, 4 wt%. A much better improvement in thermal stability of the composites could be possible by incorporating higher quantities of MWCNT. The thermal stability of PU/CNT composite was found to be improved as compared to their neat PU counterparts. TGA studies showed that PU decomposed at 300 °C, and complete degradation at 430 °C. The thermal degradation of PU matrix was successfully delayed by the addition of mCNT than that of pCNT, which indicates that the mCNT uniformly interacts with PU molecular structure. The homogeneous dispersion of the CNTs, large heat transfer due to higher thermal conductivity of PU/mCNT nanocomposites and formation and stabilization of the CNT bonded macroradicals were the main factors for enhancement of the thermal stability of PU matrix. The temperature of complete degradation of PU/mCNT-4 nanocomposites was shifted toward significantly higher temperature (~500 °C) as compared to the PU/pCNT-4 matrix (470 °C). This was attributed to the excellent thermal stability of the CNTs, the attached functional groups on the surface of the CNTs, also helped in the good interaction between MWCNTs and PU.

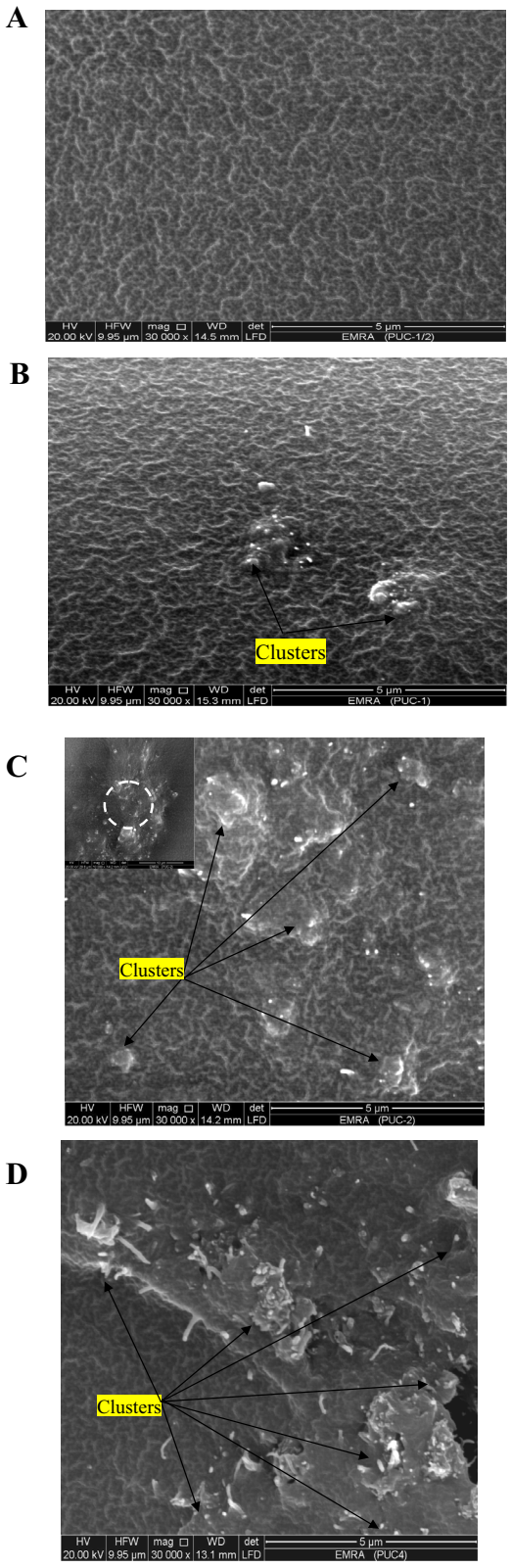

Figure 3.2 FESEM images of nanocomposite (PU/MWCNT); (A) PU/pCNT-0.5; (B) PU/pCNT-1; (C) PU/pCNT-2; (D) PU/pCNT-4.

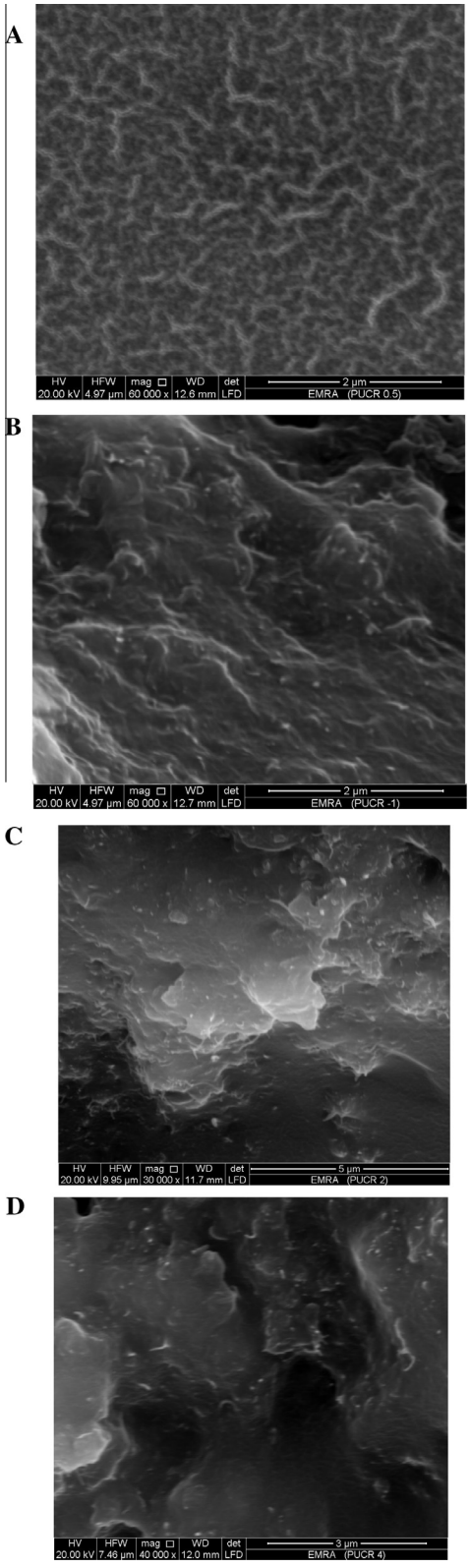

Figure 3.3 FESEM images of nanocomposite (PU/modified CNT); (A) PU/mCNT-0.5; (B) PU/mCNT-1; (C) PU/mCNT-2; (D) PU/mCNT-4.

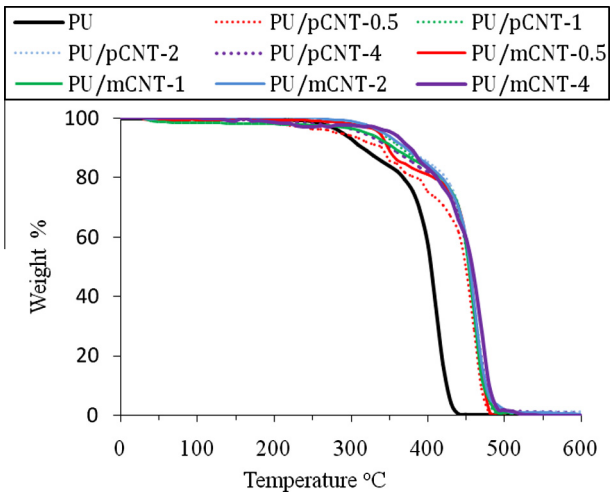

Figure 3.4 TGA thermograms of neat PU and its nanocomposites containing 0.5, 1, 2, 4 wt% of pCNT or mCNT loadings in nitrogene atmosphere.

3.3. Differential Scanning Calorimeter (DSC)

The DSC experiments revealed the glass transition (Tg) trends for pure PU, PU/pCNT and mCNT composites (Fig. 3.5). The effect of pure and surface modification CNT loading on the glass transition temperatures was analyzed by DSC. These data allowed comparing the action of pCNTs and mCNT used during nonisothermal crystallization of PU. Table 3.1 shows that the increase in Tg was observed for all CNT loading ratios. The glass transition increased with nanotube concentration and shifted toward higher temperatures with increased nanotube content. DSC measurements of PU/mCNT showed a huge increase of the Tg in the composite sample (about 41 °C). The increase of the Tg was attributed to an enhanced immobilization of polymer chains onto the CNT sidewalls [15]. The other possible reason was that well-dispersed mCNT may restrict the molecular motion of polymer chains, which could lead to an increased Tg.

The presence of active functional groups such as the hydroxyl group allowed for further covalent functionalization with polymer molecules (polymer grafting). The main approach for the covalent functionalization of CNTs with polymers had been reported: "grafting to". The grafting-to approach was based on the attachment of already preformed end-functionalized polymer molecules to functional groups on the nanotube surface via appropriate chemical reactions. DSC measurements of PU/pCNT showed a small increase (4 °C) of the Tg. This suggested some interactions of the PU to pCNTs by means of newly-formed hydrogen bonding, in spite of their tendency to agglomeration and Jung et al. For low addition of mCNT, the initial crystalline content increased substantially, while the pCNTs had minimal impact on the crystalline content. The Tg value in the mCNT-based nanocomposites exceeded than that of the pCNT-based nanocomposites by more than 20 °C. The observed difference in the effects of pCNT and mCNT in the course of nonisothermal crystallization of the PU results evidently from the higher interaction of the mCNTs with PU.

3.4. Mechanical tests

The effective enhancement in the properties of PU obtained in this study was attributed to successful dispersion of the CNTs and improved interaction between filler and matrix, which in turn, assured an efficient load transfer from the CNTs to the PU matrix phase. Mechanical properties of the casted PU/MWNT composites were investigated. All the nanocomposites showed a nonlinear elastic behavior in the low stress region and plastic deformation at higher stress. The maximum stress at break was the tensile strength [14]. Fig. 3.6(A–D) illustrates the tensile strength, elongation at break, Young's modulus and hardness in dependence on the filler content of pCNT and mCNT. For materials that exhibit a nonlinear elastic behavior, Young's modulus was determined by taking the slope of the stress–strain curve at low strain (1–5%) for all nanocomposites. Property values reported here represent averaged results for at least three specimens. The results of tensile strength, elongation at break, Young's modulus and hardness of neat PU and PU/CNTs are listed in Table 3.2. CNT reinforcement efficiency depended on the effect of the intrinsic mechanical properties, weight fractions, and aspect ratios of the nanotubes, as well as uniform nanotube distribution and matrix nanotube interfacial adhesion. Fig. 3.5(A) shows that increasing the concentration of pCNT from 0 to 4 wt% resulted in a nonmonotonic trend with a maximum around 2 wt% of CNT. At this concentration the tensile strength was nearly 2 times greater than that of neat PU. The decrease in tensile strength for a high concentration such as at 4 wt% could be ascribed to the increased frequency of localized clusters or aggregations that can be revealed in FESEM analysis of the composites at levels of higher concentration. Also, the reason might be due to the formation of CNT bundles, which might act as stress concentration regions under dynamic loading.

Table 3.2 shows summary and comparison of mechanical test of PU nanocomposites reinforcement by pCNT and mCNT.

The detailed discussion of the well-known role of nanoparticle clusters in the premature failure of inorganic filled composites was presented elsewhere. The tensile strength of PU/CNT nanocomposites containing mCNTs was enhanced by 10–41% as compared to PU/pCNTs, which could be attributed to the good dispersion of CNTs in the PU matrix and to the strong interfacial interaction between mCNT and PU. The interaction between the functionalized CNTs and the PU matrix could greatly enhance the mechanical strength of the nanocomposites. In comparison with pure PU, the PU/pCNTs with 0.5, 1, 2 and 4 wt% had about 26%, 98%, 136% and 119% increase in the elongation at break (Fig. 3.6(B)). For PU/pCNTs, a synchronous improvement in elongation at break was obtained when the pCNT content in PU matrix was lower than 4 wt%. The elongation at break of PU/pCNTs with 4 wt% decreased due to probably the restricted mobility imposed by aligned CNTs and also due to uneven dispersion of the CNTs. In PU/mCNT composite, as the mCNT content increased from 0.5 to 4 wt%, the percentage of elongation at break increased from 129% to 248.3%.

The composite with mCNT showed higher elongation at break, compared with the PU/pCNTs composite. This indicated that using mCNTs as a reinforcing additive, the

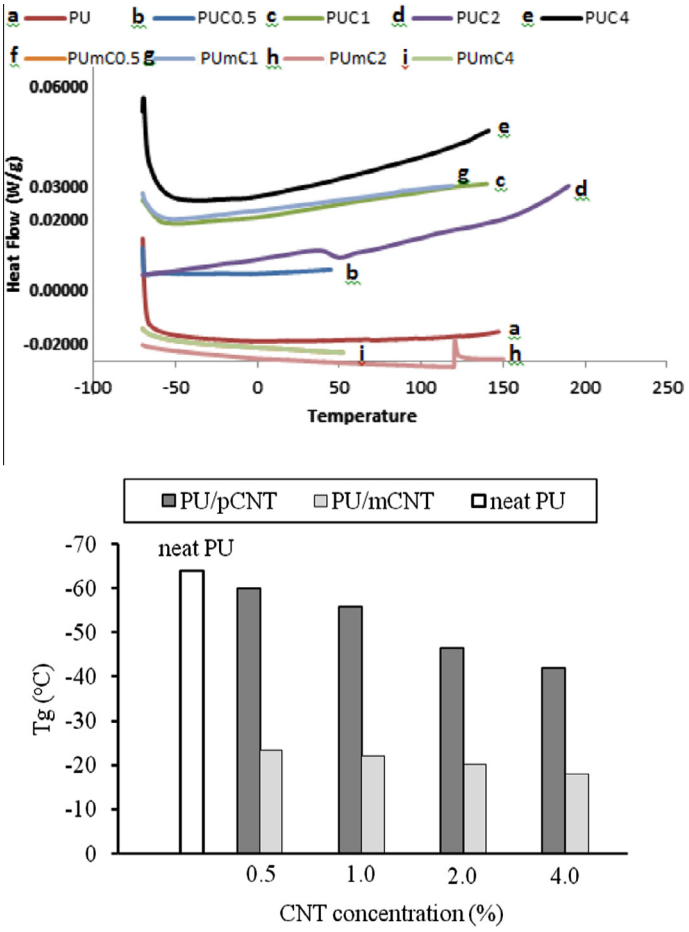

Figure 3.5 The effect of neat pCNT and modified mCNT wt% on the glass temperature Tg of polyurethane.

Table 3.1 DSC data of neat PU, PU/pCNT and PU/mCNT nanocomposites.

CNT concentration (wt%)	Tg (°C)	
	PU/pCNT	PU/mCNT
0	−64	−64
½	−60	−23.46
1	−56	−22
2	−46.5	−20.26
4	−42.05	−17.88

resistance against mechanical deformation improved without sacrificing the elongation at break for all nanocomposites filled with mCNTs up to 4 wt%. The homogeneous dispersion of mCNTs throughout the PU matrix even at higher MWCNT loading (4.0 wt%) and presence of strong interfacial adhesion between functionalized MWCNTs and the PU matrix were responsible for the significant improvement of the elongation at break of the PU/mCNT nanocomposites. The elongation at break of mCNT filled PU nanocomposites was not only significantly enhanced but also was not reduced than that of the pure CNT, it indicated that the higher wt% of mCNT loading affect the property of the nanocomposites due to the rich

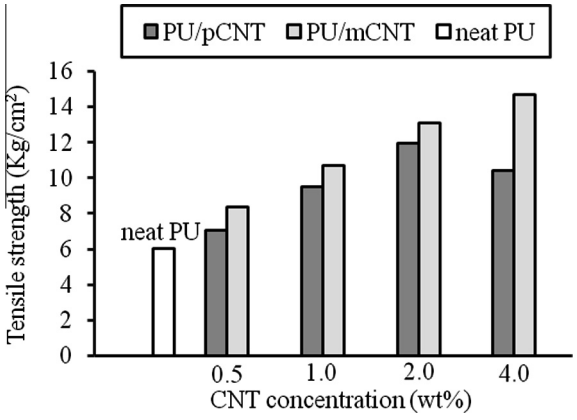

Figure 3.6(A) Comparison of tensile strength (kg/cm^2) effect of PU based on HTPB containing pCNT or mCNT for each filler content of 0.0, 1.0, 2.0 and 4.0 wt%.

dispersion of CNTs throughout the PU matrix and strong adhesive bonding with the polymer matrix.

Fig. 3.6(C) illustrates Young's modulus of neat PU and PU/CNT nanocomposites. Young's modulus of the unfilled PU is 10.17 kg/cm^2, while the nanocomposites with different

Table 3.2 Summary and comparison of mechanical test of PU nanocomposite reinforcement by pCNT and mCNT.

CNT (%)	Tensile strength (kg/cm^2)		Elongation at break (%)		Young's modulus (kg/cm^2)		Hardness (Shore A)	
	pCNT	mCNT	pCNT	mCNT	pCNT	mCNT	pCNT	mCNT
0.0	6.03	6.03	74.8	74.8	10.17	10.17	35	35
0.5	7.05	8.37	93.9	129	10.17	10.6	38	40
1.0	9.53	10.68	148.4	167.1	10.6	11.2	41	43
2.0	11.94	13.1	176.3	216.7	11.27	12.8	44	48
4.0	10.4	14.7	164.5	248.3	10.7	14.7	43	52

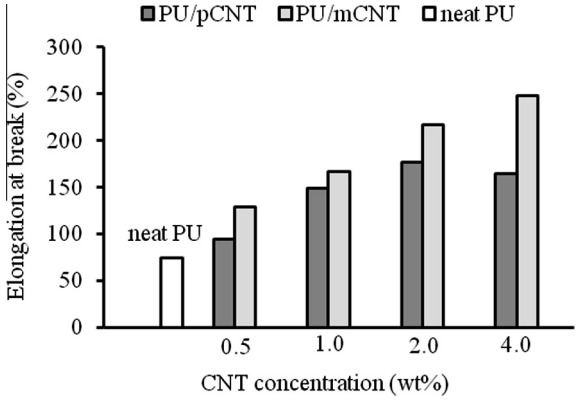

Figure 3.6(B) The effect of pCNT and mCNT concentration (wt%) on the elongation at break of PU based on HTPB.

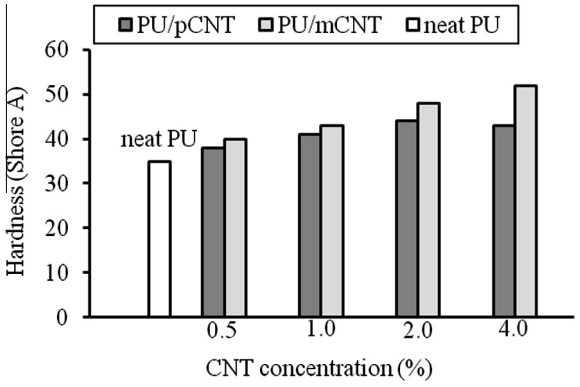

Figure 3.6(D) Hardness of neat PU and PU nanocomposites as a function of pCNT and mCNT loading.

loadings of different nanotubes showed higher modulus which is listed in Table 3.2.

Young's modulus of the PU increased up to 10.8% with the incorporation of 0.5 to 2 wt% pCNT, indicating significant enhancement in the stiffness of PUs. For pCNT at 4 wt%, there was a noticeable drop in Young's modulus compared with 2 wt% pCNT (Fig. 3.6(C)). The modulus increased linearly with pCNT concentration as expected for weight percent up to 2 wt% before beginning to saturate, possibly due to aggregation effects. Such aggregated structures tended to be less aligned by the flow, resulting in reduced mechanical properties in the final composite. Saturation occured by ~2 wt%, with this figure representing the maximum effective nanotube content. Indeed, recent modeling had shown that for

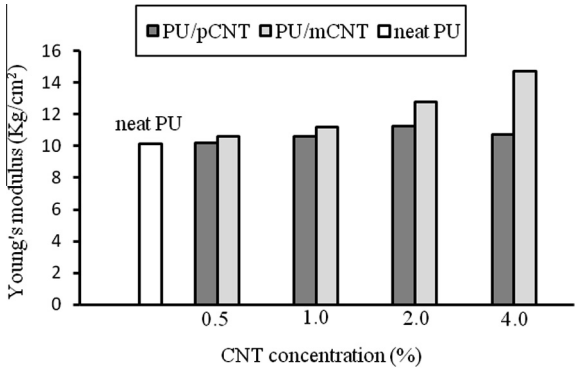

Figure 3.6(C) Young's modulus of neat PU and PU nanocomposites as a function of pCNT and mCNT loading.

nanotubes flowing in a liquid, the tendency to aggregate increased with nanotube concentration [11]. Young's modulus of PU/mCNT nanocomposites was higher compared with PU/pCNT composites. It had been shown that the functionalization of CNTs significantly improved the interfacial bonding properties between the mCNTs and PU matrix. The hydroxyl functional groups had been shown to give a stronger nanotube/polymer interaction, leading to enhanced values in Young's modulus and mechanical strength. It had been previously demonstrated that the dispersibility of MWCNTs in polymers affected the final tensile strength, where well-dispersed MWCNTs with high interfacial areas could toughen and strengthen the whole system. Better mechanical properties in tensile strength and modulus for the PU/mCNTs composites could be due to improved dispersion of the mCNTs, but also could be response to the opportunities offered by the chemically modified MWCNTs. As mentioned earlier, this was mainly due to the fact that functionalization improved both dispersion and stress transfer. [15].

Generally, the hardness was directly associated with the interconnected crosslink networks, elasticity to plasticity, strength to modulus and porosity of the polymeric matrix. The hardness of the materials indicated the inherent ability of the material to restrict the localized deformation/distortion caused by the application of external stimuli. Fig. 3.6(D) presents the hardness of the neat PU and PU nanocomposites as a function of pCNTs and mCNT concentration.

The hardness (Shore A) of pure PU was improved with the incorporation of 0.5–4 wt% pCNTs as compared to neat PU. The Shore hardness of the pure PU matrix was 35 A, whereas

PU/pCNT nanocomposites with 0.5, 1, 2 and 4 wt% pCNT loadings were 38, 41, 44 and 43A, respectively. It was concluded that the hardness of the PU/pCNT nanocomposites was significantly improved by the incorporation of pCNT as compared to neat PU. The hardness of the composites containing high concentration of pCNTs (4 wt%), decreased slightly as expected because of the poor compatibility of pCNT with PU.

From Table 2.1, it was found that, the hardness of PU/mCNT nanocomposites increased with the increasing of mCNT content. The hardness of the PU/mCNT at 0.5, 1, 2 and 4 wt% nanocomposites was 40, 43, 48 and 52A, which was incremented by about 5–21% as compared to the PU/pCNT. The increment in hardness was presumably due to the reinforcing effect of evenly dispersed mCNT as mentioned previously. The hardness of the PU/mCNT nanocomposites increased with an increase in wt% of mCNT loading. This might be most probably due to the reinforcing effect imparted by the more stable mCNTs and also due to the contribution from the strong interfacial interactions and good compatibility of mCNT with the PU matrix.

Mechanical tests showed that, compared with pure PU, the addition of modified MWCNTs (mCNT) significantly improved the tensile properties, Young's modulus and hardness of the PU matrix without sacrificing the elongation at break. This is prominently important for the applications of the PU based on HTPB development.

4. Conclusion

The functionalization of carbon nanotubes was planned in order to improve the dispersion and filler to matrix attachment. FESEM data showed that by increasing the amount of modified CNT to 4 wt%, a good dispersion of nanotubes was achieved. TGA showed that PU decomposed at 300 °C, complete degradation at 430 °C. The thermal degradation of PU matrix was delayed by the addition of modified CNT than that of unfunctionalized CNT. DSC showed that the glass transition value of the modified CNT – based nanocomposites exceeded that of unfunctionalized CNT – based nanocomposites by more than 22 °C. Mechanical tests showed that the addition of modified MWCNT improved the tensile properties, Young's modulus and hardness of the PU matrix without sacrificing the elongation at break.

References

[1] F.A. Borja, K. Umar, R. Lorena, N.C. Jonathan, M. Inaki, A.C. Maria, E. Arantxa, Influence of hard segment content and nature on polyurethane/multiwalled carbon nanotube composites, Compos. Sci. Technol. 71 (2011) 1030–1038.
[2] S.A. Abdullah, A. Iqbal, L. Frormann, Melt mixing of carbon fibers and carbon nanotubes incorporated polyurethane, J. Appl. Polym. Sci. 110 (2008) 196–202.
[3] L. Yanling, W. Chao, L. Zhanqing, Preparation, fabrication and response behavior of a HTBN/TDI/MWCNT composite sensing film by in situ dispersed polymerization, Synth. Met. 157 (2007) 390–400.
[4] F.M. Blighe, W.J. Blau, J.N. Coleman, Towards tough, yet stiff, composites by filling an elastomer with single-walled nanotubes at very high loading levels, Nanotechnology 19 (2008) 415709–415716.
[5] C. Dongyu, S. Mo, Latex technology as a simple route to improve the thermal conductivity of a carbon nanotube/polymer composite, Carbon 46 (2008) 2107–2112.
[6] C.J. Yong, J.Y. Hye, A.K. Yoong, W.C. Jae, E. Morinobu, Electroactive shape memory performance of polyurethane composite having homogeneously dispersed and covalently crosslinked carbon nanotubes, Carbon 48 (2010) 1598–1603.
[7] K.B. Aruna, K.T. Deba, Preparation, characterization and properties of acid functionalized multi-walled carbon nanotube reinforced thermoplastic polyurethane nanocomposites, Mater. Sci. Eng. B 176 (2011) 1435–1447.
[8] V.K. Lyudmyla, L.D. Raymond, K. Alina, B. Oksana, P.S. Jonathan, W.L. Andrew, V.M. Sergey, Microstructure changes of polyurethane by inclusion of chemically modified carbon nanotubes at low filler contents, Compos. Sci. Technol. 72 (2012) 865–872.
[9] R. Mohan, A.M. Shanmugharaj, H.R. Sung, J. Subha, Influence of metal nanoparticle decorated CNTs on polyurethane based electro active shape memory nanocomposite actuators, Mater. Chem. Phys. 129 (2011) 925–931.
[10] S.A. Shokry, A.K. El Morsi, M.W. Saba, R.R. Mohamed, H.E. El Sorogi, EGYJP 23 (2014) 3.
[11] P.C. Ma, J.K. Kim, B.Z. Tang, Functionalization of carbon nanotubes using a silane coupling agent, Carbon 44 (2006) 3232–3238.
[12] S. Hao, Z. Zhao-Zhu, M. Xue-Hu, Surface-modified carbon nanotubes and the effect of their addition on the tribological behavior of a polyurethane coating, Eur. Polymer J. 43 (2007) 4092–4102.
[13] X. Jiawen, Z. Zhen, S. Wenhui, Z. Dongsheng, W. Xinling, Microstructure and properties of polyurethane nanocomposites reinforced with methylene-bis-orthochloroaniline-grafted multi-walled carbon nanotubes, Compos. A 39 (2008) 904–910.
[14] C. Wei, T. Xiaoming, L. Yuyang, Carbon nanotube-reinforced polyurethane composite fibers, Compos. Sci. Technol. 66 (2006) 3029–3034.
[15] S. Zdenko, T. Dimitrios, P. Konstantinos, G. Costas, Carbon nanotube–polymer composites: chemistry, processing, mechanical and electrical properties, Prog. Polym. Sci. 35 (2010) 357–401.